Proceedings of the ASME 2014 Dynamic Systems and Control Conference
DSCC2014
October 22-24, 2014, San Antonio, Texas, USA

DSCC2014-6322

ADAPTIVE REPETITIVE CONTROL USING A MODIFIED FILTERED-X LMS ALGORITHM

Behrooz Shahsavari
Department of Mechanical Engineering
University of California
Berkeley, California 94720
Email: behrooz@berkeley.edu

Ehsan Keikha
Department of Mechanical Engineering
University of California
Berkeley, California 94720
Email: keikha@berkeley.edu

Fu Zhang
Department of Mechanical Engineering
University of California
Berkeley, California 94720
Email: shallen@berkeley.edu

Roberto Horowitz
Department of Mechanical Engineering
University of California
Berkeley, California 94720
Email: horowitz@berkeley.edu

ABSTRACT

In this paper we develop a modified filtered-x least mean squares (MFX-LMS) method to synthesis an adaptive repetitive controller for rejecting periodic disturbances at selective frequencies. We show how a MFX-LMS algorithm can be utilized when the reference signal is deterministic and periodic. A new adaptive step size is proposed with the motivation to improve the convergence rate of the MFX-LMS algorithm and fade the steady state excess error caused by the variation of estimated parameters in a stochastic environment. A novel secondary path modeling scheme is proposed to compensate for the modeling mismatches online. We further discuss the application of this adaptive controller in hard disk drives that use Bit Patterned Media Recording. Finally we present the results of comprehensive realistic numerical simulations and experimental implementations of the algorithms on a hard disk drive servo mechanism that is subjected to periodic disturbances known as repeatable runout.

INTRODUCTION

Repetitive control is used to cancel disturbances or execute commands which are periodic in time. This type of control methodology has been widely used for the applications in which a trajectory should be followed repeatedly or attenuation of a periodic disturbance is desired. For instance, a robot link that is performing a periodic motion in the work space is a dynamic system that is subject to periodic gravity force and torque. Hard disk drive servo system, satellite attitude control, helicopter forward flight, orbital stabilization of under-actuated systems, and rotating machinery are other applications of repetitive control.

The concept of repetitive control was first introduced in 1980's and early works include [1, 2]. This type of controllers are typically classified into either internal model based or external model based compensators [3]. The key distinction between these two structures is that in an internal model based controller a periodic signal generators is embedded [4], while the latter structure views the cancellation signal as being injected from outside of the plant/controller feedback loop [5].

In this paper we pursue employing modified filtered-x least

mean squares (MFX-LMS) algorithm – which can be categorized as an external model based method – to develop an adaptive repetitive controller. Least mean squares (LMS) as a stochastic gradient descent method was first developed by Widrow and Hoff [6] in 1960's and began to flourish due to its simplicity and stable behavior when implemented with finite-precision arithmetic [7]. However, this algorithm is generally unstable when its output enters to a dynamic system at a point which is distinct from the injection point of reference signal. The reason behind this instability behavior is that the error signal is not correctly "aligned" in time with the reference signal [8]. The concept of using a secondary path in the adaptation algorithm to solve this problem was later introduced independently by Burgess [9], and Widrow [10]. This technique is called filtered-x LMS (FX-LMS) and it appears to be very robust to the mismatches between the model used in the secondary path and the real system [11]. However, the convergence rate of FX-LMS algorithm when the secondary path exists is slower than the simple LMS in the absence of secondary path. Bjarnason [12] and Kim [13] proposed a modification in the update equation of FX-LMS to adapt the algorithm to the standard LMS method when the secondary path model is identical to the real system. This algorithm is known as MFX-LMS and has been extensively used in active noise cancellation. Motivated by the fact that MFX-LMS algorithm has benefit of being robust as FX-LMS, and fast as LMS algorithm, we pursue this method to synthesis an adaptive repetitive controller for rejecting periodic disturbances at desired frequencies. We show how a MFX-LMS algorithm can be utilized when the reference signal is deterministic and periodic. A new variable step size is proposed with the motivation to improve the convergence rate of the MFX-LMS algorithm and fade the steady state excess error caused by the variation of estimated parameters in a stochastic environment. We also propose an online secondary path modeling scheme to compensate for the mismatch between the plant model embedded in the adaptive controller and the real plant dynamics.

As mentioned earlier, one application of repetitive control is disturbance rejection in hard disk drives (HDD). The servo control mechanism of hard disk drives are usually subject to periodic disturbances that are due to the imperfection in both fabrication and assembly processes. A great deal of research effort has been focused on bit patterned media recording (BPMR) – a method in which data is stored in an array of single-domain magnetic particles – in recent years since it is recognized as a potential breakthrough method to increase the areal density of hard disk drives significantly [14, 15]. Later in the paper, we will discuss the application of the proposed repetitive control in BPMR and finally we present the results of comprehensive numerical simulations and experimental implementation of the algorithms on a hard disk drive that is subjected to periodic disturbances known as repeatable runout.

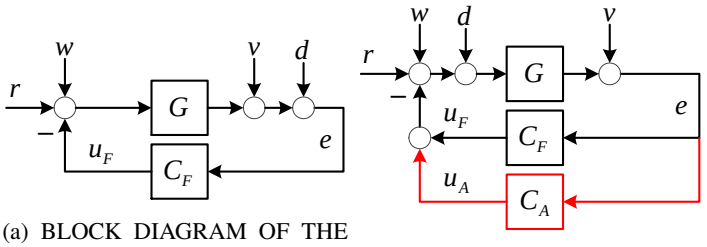

(a) BLOCK DIAGRAM OF THE SYSTEM WITH NOISES AND PERIODIC DISTURBANCE.

(b) PLUG-IN ADAPTIVE REPETITIVE CONTROLLER.

FIGURE 1: Control architecture

ADAPTIVE CONTROL SYNTHESIS

The block diagram of the closed loop system of interest that is subject to periodic disturbance is shown in Fig. 1a. The feedback system is composed of the linear time invariant (LTI) plant G and a LTI feedback controller C_F. The signals r, w, v, d and e are the reference, input noise, output noise, periodic disturbance and error respectively. Note that we do not necessarily need to consider d entering the system on the output side of the plant since it is unknown and the system is linear; hence, it is possible to consider the periodic disturbance at any other point, or multiple points in the closed loop system.

We aim to compensate for the effect of disturbance d on error signal e by adding an adaptive controller, say C_A, in a *Plug-in* fashion as it is shown in Fig. 1b. Note that, by the same argument as stated above, the error signal can be defined anywhere in the closed interconnection of G and C_F. Without loss of generality, throughout this paper we assume that the disturbance and error signals are defined according to Fig. 1b.

We decompose the disturbance signal as a sum of sinusoids by considering the Fourier transformation of d at any time step k (i.e. d_k)

$$d_k = \sum_{i=1}^{n} \left[a_i \left(\alpha_i \sin\left(\omega_i k T\right) \right) + b_i \left(\alpha_i \cos\left(\omega_i k T\right) \right) \right] + \eta_k \quad (1)$$

$$= \theta^T \phi_k + \eta_k \quad (2)$$

where ω_i's denote the frequencies of those components that are desired to be removed from the spectrum of e, η_k denotes the summation of components at other frequencies, T is the sampling time of the discrete system, and

$$\theta^T := [a_1, \cdots, a_n, b_1, \cdots, b_n] \quad (3)$$

$$\phi_k^T := [\alpha_1 \sin\left(\omega_1 k T\right), \cdots, \alpha_n \sin\left(\omega_n k T\right), \alpha_1 \cos\left(\omega_1 k T\right), \cdots, \alpha_n \cos\left(\omega_n k T\right)] \cdot \quad (4)$$

Here, ϕ_k is a known reference signal since both ω_i's and α_i's are selected values. The control objective is to estimate the parame-

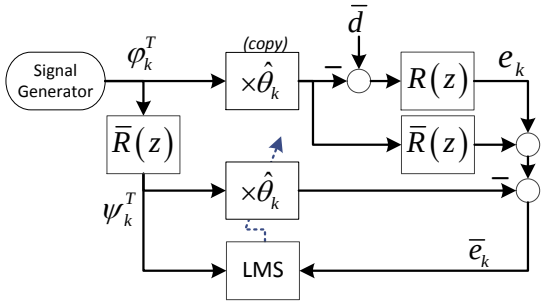

FIGURE 2: MODIFIED FILTERED-X LMS SCHEME

ter vector θ in an adaptive way and construct the control signal u_A at time step k

$$u_{A,k} = \hat{\theta}_k^T \phi_k \tag{5}$$

where $\hat{\theta}_k$ denotes the estimated parameter vector at time step k.

We use a modified Filtered-x LMS structure with ϕ_k as the reference signal to estimate the parameters vector adaptively. This method differs from most preceding ones used in active noise cancellation (ANC) in that the reference signal is a known vector here, while in ANC, it is usually a vector of delayed measurements from a sensor (e.g. a microphone). The parameter adaptation structure is shown in Fig. 2. The estimated parameters vector $\hat{\theta}_k$ is updated by

$$\hat{\theta}_{k+1} = \hat{\theta}_k + \mu_k \psi_k \bar{e}_k \tag{6}$$

where μ_k is a novel variable step size that will be introduced in the following subsection. Vector $\psi_k \in \mathbb{R}^{2n}$ is known and generated by filtering the reference signal ϕ_k element-wisely through the discrete time nominal transfer function, say $\bar{R}(z)$, from $-u_A$ to e. Let $\psi_{i,k}$, $\phi_{i,k}$, r_k be respectively the i-th element of ψ_k, ϕ_k and the impulse response of $\bar{R}(z)$ at time step k

$$\psi_{i,k} = (\phi_i * r)_k = \sum_{\tau=0}^{k} \phi_{i,\tau} r_{k-\tau}$$

where $*$ represents the convolution operator and we have assumed that all signals are zero for $k < 0$. The transfer function $\bar{R}(z)$ for the system under study is

$$\bar{R}(z) = \frac{\bar{G}(z)}{1 + C_F(z)\bar{G}(z)} \tag{7}$$

where $\bar{G}$ is a nominal model for the actual plant G. If the error signal e is defined in a different way, the transfer function $\bar{R}(z)$ should be modified accordingly. Since this system is linear, the steady state filtered reference can be calculated simply by

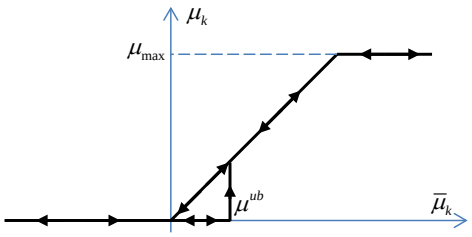

FIGURE 3: VARIABLE STEP SIZE WITH HYSTERESIS BEHAVIOR.

$$\psi_{i,k} = \begin{cases} m_i \alpha_i \sin(\omega_i k T + \delta_i), & i \in \{1, \cdots, n\} \\ m_i \alpha_i \cos(\omega_i k T + \delta_i), & i \in \{n+1, \cdots, 2n\} \end{cases} \tag{8}$$

$$m_i = \| \bar{R}\left(e^{j\omega_i T}\right) \|_2, \quad \delta_i = \angle \bar{R}\left(e^{j\omega_i T}\right). \tag{9}$$

Here, $\|x\|_2$ and $\angle x$ denote the magnitude and phase of a complex number x. The variable $\bar{e}_k$ in (6) is called *auxiliary error* and it is defined by

$$\bar{e}_k := e_k + \bar{R}\left[u_{A,k}\right] - \hat{\theta}_k^T \psi_k \tag{10}$$

where $\bar{R}\left[u_{A,k}\right]$ is the output of filter $\bar{R}(z)$ at time step k when its input is u_A.

Remark 1. *Note that when* $R(z) = \bar{R}(z)$ *the* auxiliary error *is*

$$\begin{aligned} \bar{e}_k &= R\left[\phi_k^T \theta + \eta_k - \phi_k^T \hat{\theta}_k\right] + R\left[\phi_k^T \hat{\theta}_k\right] - \psi_k^T \hat{\theta}_k \\ &= \psi_k^T \left(\theta - \hat{\theta}_k\right) + \xi_k \end{aligned} \tag{11}$$

where $\xi_k := R[\eta_k]$ *can be thought of as noise, and accordingly the adaptive algorithm is in the standard LMS form rather than MFX-LMS. This illustrates the intuition behind using the secondary path in the MFX-LMS algorithm – i.e. using the* auxiliary error *rather than the actual error.*

Remark 2. *It is well known that the convergence rate of the LMS algorithm depends on the eigenvalue spread of the reference correlation matrix [16]. This fact with remark 1 suggests that the values of* α_i*'s in* (3) *should be chosen such that the amplitude of all sinusoidal elements in* (8) *are equal – i.e.* $\alpha_i \propto \frac{1}{m_i}$.

Variable Step Size: μ_k

The step size in update equation of adaptive algorithms has a significant role in determining the transient and steady state behavior of the algorithms. It is well known that the choice of step

size reflects a trade off between the steady state misadjustment and convergence rate [17]. In a stochastic environment, a large value of step size results in fast convergence of estimated parameters and large steady state misadjustment due to fluctuation of the estimated parameters around the optimal values which is caused by the contaminating noises.

Our key idea to define a variable step size is that as the estimated parameters get closer to the real ones, the step size becomes smaller and the parameters will be frozen in time when a certain desired performance (in terms of mean squared error) is attained. This removes the excess error from the output and results in smaller steady state errors. It is also required that the step size becomes positive (i.e. adaptation starts again) whenever the error becomes large (e.g. the disturbance profile or the system dynamics changes). We propose equation (12) for such a step size since this formulation satisfies all the aforementioned conditions and it is easy to compute in real-time.

$$V_k^h = V_{k-1}^h + \frac{1}{h}\left(\bar{e}_k^2 - \bar{e}_{k-h+1}^2\right) \tag{12a}$$

$$\bar{\mu}_k = \rho\left(V_k^h - V^d\right) \tag{12b}$$

$$\mu_k = \begin{cases} min(\bar{\mu}_k, \mu_{max}) \text{ if } (\bar{\mu}_k > 0 \wedge \mu_{k-1} > 0) \\ \qquad\qquad \vee(\bar{\mu}_k > \mu^{ub}) \\ 0 \qquad\qquad \text{otherwise} \end{cases} \tag{12c}$$

Here, V_k^h indicates the *auxiliary error* power in a finite window of length h, and V^d is the desired value for such a measure that should be selected by the designer according to the application. For instance, when η_k in (1) is zero, and both w and v in Fig. 1b are white noises, V_d should be chosen to be larger than the $\mathscr{H}_2$ norm of the closed loop system from the inputs to e. When real measurements of error signal e are available to the designer at the design stage, an appropriate value of V^d can be practically chosen by summing the power spectrum (e.g. by using a periodogram) of the error at all frequencies excluding w_i's.

Constant ρ in (12) is a positive scalar gain, and μ_{max} denotes the maximum step size to guarantee the convergence of the second moment of error. It is well known that a sufficient condition for guaranteeing mean squared error (MSE) convergence is to choose $\mu_{max} \leq \frac{2}{3\psi_k^T\psi_k}$ for all values of k [18]. Since V_k^h is calculated by averaging on a finite history of the squared auxiliary error, it is not exactly equal to the auxiliary error variance. As a results, the system may show *chattering* behavior around the switch line (i.e. $V_k^h = V^d$) if $\bar{\mu}_k$ is used directly as the step size. To avoid this, we add a hysteresis behavior to the step size by adding a deadband around the switch line. The deadband width will be defined by μ^{ub} as is defined in (12c), and illustrated in Fig. 3.

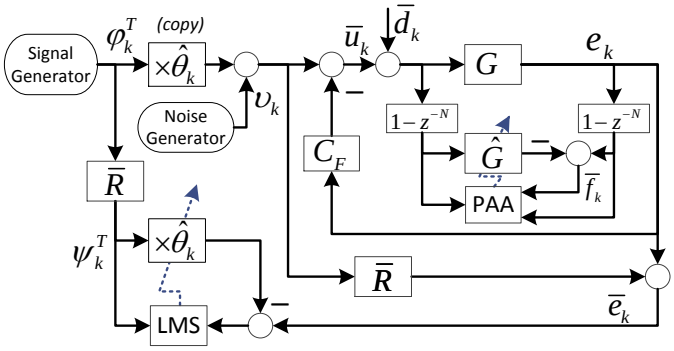

FIGURE 4: ADAPTIVE CONTROLLER WITH SECONDARY PATH MODELING

SCHEDULING THE ADAPTATION

In the lack of a priori knowledge about the parameter values, the adaptation algorithm is usually initiated by zero parameters which can result in large values of transient error. The number of parameters is another factor that affects the transient error in that more inaccurate initial parameters result in a larger transient error in general. This is not desirable in many applications since it may either damage the system or waste energy. We propose a simple modification to (6), in order to schedule the adaptation of different parameters such that at each moment only a certain number of parameters are being updated and, as a result, the magnitude of the transient error is reduced. Let $\hat{\theta}_k^i$ be the ith element of $\hat{\theta}_k$, then the modification in the parameter adaptation algorithm can be made through

$$\hat{\theta}_{k+1}^i = \hat{\theta}_k^i + \gamma_k^i \mu_k \psi_k^i \bar{e}_k \tag{13}$$

where γ_k^i is a binary variable that is one when the ith parameter should be updated and zero otherwise. We will be returning to this idea again in the last section when we apply the proposed variable step size with this modification to a hard disk drive servo system.

ONLINE SECONDARY PATH MODELING

The performance of the MFX-LMS algorithm may suffer from the mismatch between the model used in the secondary path, $\bar{R}(z)$, and the actual transfer function, $R(z)$. A sufficient condition for robustness to the secondary path modeling mismatch is that the phase difference between these two systems should be less than 90 degrees when the step size is small [19] – i.e. $Re\left[\bar{R}(z)/R(z)\right] > 0$. In this section we present a novel adaptive modeling scheme, as is illustrated in Fig. 4, to compensate for the secondary path mismatch.

In the figure, $\hat{G}(z)$ is the estimated plant model and **PAA** denotes the parameter adaptation algorithm. An important dis-

tinction between this architecture and the previous works is that we take the advantage of knowing the feedback controller $C_F(z)$ and only identify the plant, while in other works [20, 21], modeling of the closed loop system $R(z)$ is considered. Therefore, the number of parameters in this approach is less compared to the previous works.

There are two cases to be considered here. First, *Initialization*, a period in which the two paths, adaptive repetitive control path and modeling path, are running separately and the estimated plant at time step k, say $\hat{G}_k(z)$, is not used in the other adaptive algorithm. Second, the case in which $\bar{R}(z)$ is being updated by the estimated plant model using $\bar{R}_k(z) = \hat{G}_k(z) / \left(1 + C_F(z)\hat{G}_k(z)\right)$.

Initialization: During this period the modeling path does not affect the adaptive controller since the estimated plant model is not used in the control path. From the adaptive control point of view, the only difference between this case and Fig. 2 is the new noise, υ_k, injected to the system. Note that since the reference signal ϕ_k is deterministic, the noise is uncorrelated with the reference signal and the parameters will be unbiased as long as the noise is zero mean. We can also show that the adaptive control will not affect the modeling path since the input to the **PAA** is the summation of the feedback control, adaptive control, and the periodic disturbance. We can think of the summation of the first two terms as a known reference signal and accordingly we only need to filter out the periodic disturbance in order to have an unbiased estimation of the parameters. A method to achieve this goal is proposed in the following subsection.

Filtering Periodic Disturbance

Let $G(q^{-1})$ be the transfer function of G represented by the one step delay operator q^{-1}

$$G\left(q^{-1}\right) = \frac{B\left(q^{-1}\right)}{A\left(q^{-1}\right)} = \frac{b_0 + b_1 q^{-1} + \cdots + b_{n_g} q^{-n_g}}{1 + a_1 q^{-1} + \cdots + a_{n_g} q^{-n_g}}.$$

The error signal in Fig. 4 is $e_k = \theta_g^T \phi_{g,k} + d_{g,k}$ where

$$\theta_g^T := \left[a_1, \cdots, a_{n_g}, b_0, \cdots, b_{n_g}\right] \tag{14}$$

$$\phi_{g,k}^T := \left[e_{k-1}, \cdots, e_{k-n_g}, \bar{u}_k, \cdots, \bar{u}_{k-n_g}\right] \tag{15}$$

$$d_{g,k} := G\left[\bar{d}_k\right]. \tag{16}$$

Depending on the relative degree of numerator and denumerator of G, say n_d, we know that $b_i = 0$ for $i \in \{0, \cdots, n_d\}$. However, here we do not make any assumptions on n_d and consider the general case. Note that $d_{g,k}$ is periodic in steady state since $\bar{d}_k$ is periodic and $G\left(q^{-1}\right)$ is a LTI system. In the remaining of the paper we assume that $d_{g,k}$ is periodic and this fact leads us to filter both e_k and $\phi_{g,k}$ through $1 - q^{-N}$ and define

$$\begin{aligned} \bar{f}_k &:= (e_k - e_{k-N}) - \hat{\theta}_{g,k}\left(\phi_{g,k} - \phi_{g,k-N}\right) \\ &= \tilde{\theta}_{g,k}^T \psi_{g,k} \end{aligned} \tag{17}$$

where $\psi_{g,k} = \phi_{g,k} - \phi_{g,k-N}$. Note that (17) gives a suitable representation of an "error" variable to be used in an adaptive algorithm. Depending on how the system is contaminated by noises, a proper adaptive algorithm can be selected to identify the system parameters by using the error variable $\bar{f}_k$ and reference signal $\bar{\phi}_{g,k}$.

Simultaneous Adaptation: Now let us consider the second case in which $\bar{R}(z)$ is updated by $\bar{R}_k(z) = \hat{G}_k(z) / \left(1 + C_F(z)\hat{G}_k(z)\right)$. With the same argument as the initialization period, the adaptive control path does not affect the modeling path and the estimated plant parameters will converge if the filtering method is applied to remove the periodic disturbance. On the other hand, the adaptive control path will not converge as long as the updated transfer function $\bar{R}(z)$ has more than 90 degrees phase error. As a result when the initial parameters of $\hat{G}$ are not accurate, we expect that the adaptive control path becomes unstable and its estimated parameters diverge quickly. Although the adaptive control path becomes stable eventually – once the plant parameters get close enough (in terms of phase error) – this behavior is not desirable in many applications since the transient error may be very large, and accordingly the adaptive control requires a long time to correct the diverged parameters.

We thus suggest using the initialization period prior to the simultaneous adaptation when a good knowledge of the plant parameters is not available.

Remark 3. *In many applications the plant dynamics is well known at a frequency range, say Ω. If such information is available, the frequency components of disturbance can be categorized into two sets $I_1 = \{i | \omega_i \in \Omega\}$ and $I_2 = \{i | \omega_i \notin \Omega\}$. The adaptation of parameters $\hat{\theta}^i, i \in I_1$ and plant parameters can be done simultaneously since the plant model is exact at that region. This can be done by choosing*

$$\gamma_k^i = \begin{cases} 0 & i \in I_2 \text{ and } k \leq P \\ 1 & \text{otherwise} \end{cases} \tag{18}$$

where P denotes the length of initialization period required for secondary path modeling.

APPLICATION TO BPM HARD DISK DRIVES

Accurate and precise control of the read/write head position in a hard disk drive (HDD) is performed by a nano positioning

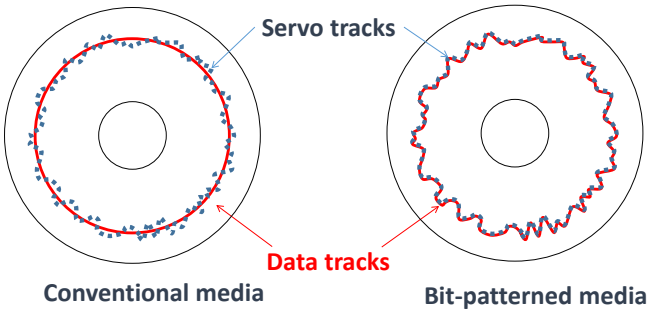

FIGURE 5: SERVO TRACK IN CONVENTIONAL AND BIT PATTERNED MEDIA HDD.

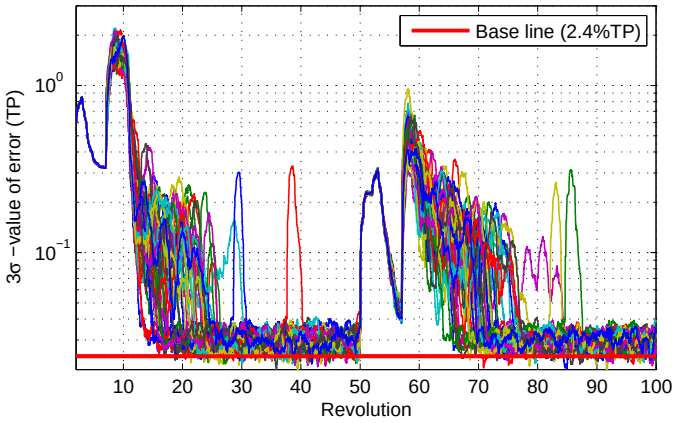

FIGURE 6: 3σ OF ERROR FOR DIFFERENT PLANTS AND TWO PROFILES (SIMULATION STUDY).

servomechanism. This servomechanism is a feedback system consisting of a sensing element that measures the displacement of the head, a controller and one (two) actuator(s) [22]. The control strategy in conventional HDDs that use continuous media is distinct from BPMR in that data is written on concentric circular tracks in the former one, while in BPMR data should be written on trajectories with special unknown shapes which are created by lithography on the disk. A schematic of the ideal trajectory for these two types of magnetic recording is shown in Fig. 5. The desired trajectory to be followed in BPR is determined by a servo track which is written on the disk and its deviation from an ideal circle is called repeatable runout (RRO). Indeed, we can think of the RRO as a periodic trajectory that should be followed by the read/write head and accordingly model the servo mechanism similar to the system shown in Fig. 1a. By this analogy, disturbance d will present the RRO with negative sign and following the RRO is equivalent to compensating for the effect of disturbance d on error e.

Repeatable runout is caused by both imperfection in fabrication – e.g. e-beam and imprint error – and mechanical defects such as disk deformation by clamp and eccentricity of disk. All of these defects results in a periodic profile that only contains frequency components at the disk spinning frequency and its harmonics up to the Nyquist frequency of the controller,

$$d_k = \sum_{i=1}^{N/2} a_i \sin(i\omega_0 kT) + b_i \cos(i\omega_0 kT) \cdot \qquad (19)$$

Here, ω_0 is the spinning frequency of the disk (in rad/s), which is usually called the fundamental frequency, T is the sampling time of controller and $N = \frac{2\pi}{\omega_0 T}$ is the number of measurements attained during one revolution of the disk.

Control design for BPR is challenging since the RRO profile is unknown and its spectrum contains many (e.g. 200) frequency components that can spread beyond the feedback system bandwidth; therefore, the RRO will be amplified by the feedback system. Moreover, the large number of frequency contents raises computational burden in the controller. Accordingly, the servo control methodologies used for conventional drives [3, 23–25] cannot be applied to BPR.

Simulation Study

Comprehensive numerical simulations are conducted to verify the effectiveness of the proposed algorithm. Since BPMR HDDs have not been released yet we do a simulation study to validate the effectiveness of our proposed algorithm for this type of hard disk drives. We expect that the actuator and contaminating noises will be similar in both types of magnetic recording, and so we model the dynamics and noises of the system based on the data collected from a 2.5-inch conventional hard disk drive that is provided by HGST, a Western Digital company. However, the RRO profiles are distinct since the fabrication processes are different. We use the RRO data from a prototype BPM hard disk drive that is provided by Seagate to create an artificial RRO profile for our simulations.

Figure. 1b shows a succinct representation of the servo system with adaptive repetitive controller C_A. LTI systems G and C_F denote the voice coil motor (VCM) – the actuator that moves the read/write head – and the built-in track following controller of the servo system. Noises w and v respectively represent the undesired airflow force (windage), and the summation of non-repeatable runout and measurement noise. Note that if we ignore these two noises the error is zero if the head position follows the RRO – e.g. the case that is shown in the right schematic in Fig. 5. In this simulation, w, and v are colored noises with proper rational power spectral densities which are modeled based on real data. Similarly, G and C_F are modeled based on the frequency response of the system that is measured by experiments. The transfer function $G(z)$ is created by discretization of a continu-

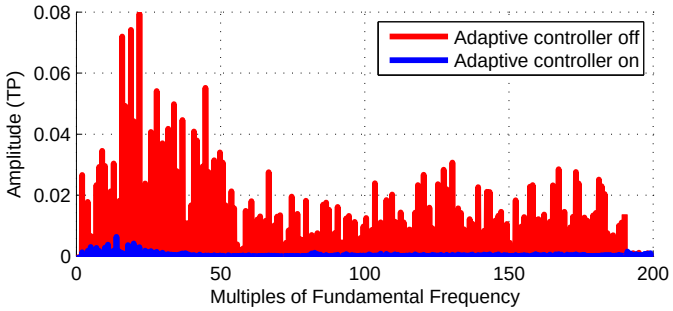

FIGURE 7: SIMULATED FOURIER TRANSFORM MAGNITUDE OF STEADY STATE ERROR IN TRACK PITCH (TP)

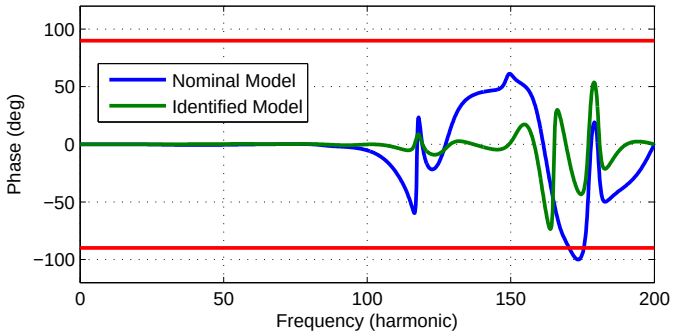

FIGURE 8: PHASE MISMATCH BETWEEN THE PLANT MODELS AND ACTUAL PLANT (SIMULATION STUDY).

ous time system – denoted as $G(s)$ – that includes second order resonance modes and a first order low pass filter that corresponds to the electronic amplifier of the VCM.

$$G(s) = G_1(s)\left[G_2(s) + \cdots + G_7(s)\right]$$
$$G_1(s) = \frac{g_1}{s - w_1}$$
$$G_i(s) = \frac{g_i}{s^2 + 2\zeta_i w_i s + w_i^2}\ ,\quad i \in \{2, \cdots, 7\}$$

Parameters g_i's, w_i's and ζ_i are determined by fitting the frequency response of $G(s)$ to the measured data. 2% uncertainty is added to the nominal values of VCM resonance frequencies to create 50 uncertain plant dynamics. Performance of the proposed method is tested on each individual plant model and the results are presented here.

Performance of the system is quantified in terms of the 3σ value of error, which is "3 times the standard deviation of error". Fig. 6 shows approximated 3σ value of position error signal (PES) calculated by averaging on root mean square (RMS) of PES in one revolution. Different colors on the figure correspond to the performance of different uncertain plant models simulated for 100 revolutions of the disk. In the first 50 revolutions the head is moving on a mid-diameter (MD) track and so the controller is trying to follow RRO on MD. As can be seen from the figure, all plants have reached steady state performance by 50 revolutions. RRO profile is changed to an outer-diameter (OD) track after revolution 50. In both cases in order to decrease the transient error, the adaptation for harmonics $1-80$ starts first and for harmonics $81-190$ starts after 7 revolutions. As can be seen from the figure, the 3σ of error is approximately 3% of track pitch in all cases (both tracks and all of the plants). This result is impressive if we compare it to the baseline (perfect RRO following) which is 2.4% of track pitch. The magnitude of error Fourier transform before and after using the adaptive repetitive controller is shown in Fig. 7. Since we have chosen a desired performance, V^d, larger than the minimum variance (attained by perfect tracking), the frequency components of error at harmonics of fundamental frequency are not exactly zero. The left over, which is larger between harmonic 10 and 50, corresponds to the difference between V^d and variance of error in perfect tracking.

Finally we have simulated the proposed secondary path modeling scheme to identify the plant dynamics of VCM online. Figure 8 shows the phase mismatch between the nominal plant model and the actual one, which is more than 90 degrees (in magnitude) at high frequencies. A recursive least squares algorithm with the proposed filtering method is used to identify the plant parameters. The phase error for the identified systems is shown in Fig. 8. This result is the same for both *initialization* and *simultaneous adaptation*. However, the transient error for simultaneous adaptations is significantly larger since the adaptive controller is unstable in early revolutions.

Comparison with Other Popular Adaptive Methods

In this section, our proposed method is compared with recursive least squares, standard LMS and normalized LMS in terms of performance and implementation difficulty. Note that in all of these algorithms the update equation, (6), is the same and the only distinction is the step size μ_k.

Recursive Least Squares (RLS) The step size is a $2n \times 2n$ matrix that should be calculated recursively by

$$\mu_{k+1} = \frac{1}{\gamma}\left(\mu_k - \frac{\mu_k \psi_k \psi_k^T \mu_k}{\gamma + \psi_k^T \mu_k \psi_k}\right) \tag{20}$$

where $\gamma \in [0,\ 1]$ is known as the *forgetting factor*, and $\gamma = 1$ corresponds to the standard RLS algorithm. The number of both multiplications and additions needed for (20) is $\mathcal{O}\left(4n^2\right)$. The time complexity of our proposed method with the variable step size is linear in $2n$. Since in a BPM HDD $2n$ is $\mathcal{O}\left(10^2\right)$, the time

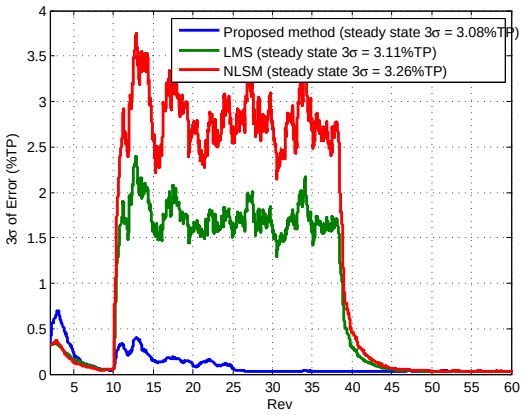

FIGURE 9: PERFORMANCE OF THE PROPOSED METHOD, LMS AND NLMS (SIMULATION STUDY)

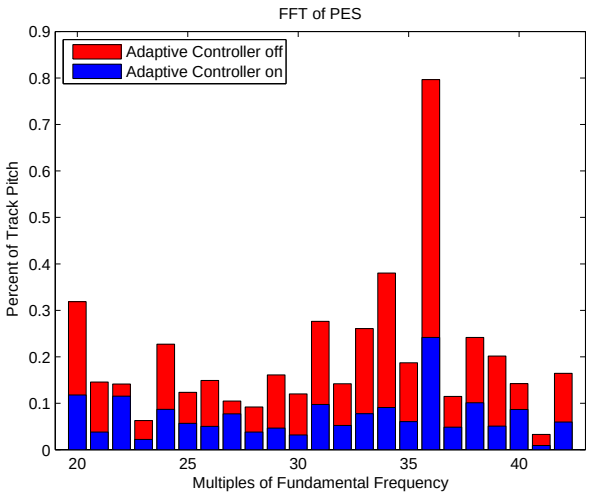

FIGURE 10: CLOSED LOOP ERROR SPECTRUM OF 23 MAJOR COMPONENTS OF RRO (EXPERIMENTS)

complexity of RLS is approximately two orders of magnitude larger than the proposed method.

Standard and Normalized LMS The step size in both standard and normalized LMS (NLMS) algorithms does not depend on the error behavior. Accordingly, they either suffer from large excess error or slow convergence. Figure 9 shows the performance in terms of 3σ value of error for these two methods and our proposed algorithm. In all cases, the adaptation of harmonics $1-80$ and $81-190$ is started from revolution 2 and 10 respectively. As can be seen in the figure, the excess error caused by high frequency contents in LMS and NLMS between revolution 10 and 30 is considerably large. Since the step sizes of LMS and NLMS are not adaptive, we need to turn the adaptation off manually. This is done at the beginning of revolution 37, that has resulted in a drastic decrease in error. On the other hand, since the proposed method has adaptive step size, it does not need any manual switching. Our method reaches the desired performance (e.g. 3% of track-pitch (TP)) after 27 revolutions, and its transient error is significantly smaller since the step size decreases as the parameters converge to the real values.

IMPLEMENTATION RESULTS

Simulation results in the previous section confirmed that the designed controller achieves the desired performance level in the presence of a broad range of RRO component in the PES. Experimental results are presented in this section, which confirm the validity of analytical and simulation results. The experimental setup consists of a commercial HDD (provided by HGST, a Western Digital company), a digital signal processor (DSP-OMAPL138), and a digital to analog converter (DAC - AD5441). Modifications were made in the firmware of the HDD to send out PES via Serial Peripheral Interface (SPI) Bus to the DSP, which run the adaptation and calculate the control action. In our setup we do not change or disable the HDD internal controller. Rather, the adaptive RRO tracking controller is designed as a "plug-in controller". The actuation signal is injected to the linear amplifier of the VCM through the DAC board. Since the internal HDD controller already compensates the low frequency part of the RRO, the major observed RRO peaks are located in the mid-frequency range. We designed an adaptive controller to attenuate the 23 major PES RRO components which are from harmonic numbers 20 to 42. Since the plant dynamics is well known in this frequency range the secondary path modeling algorithm is not implemented. Instead, we use a second order system that is fitted to the actual plant dynamics – obtained by measurements – accurately in mid frequency range. Figure. 10 compares the Fourier transform magnitude of the PES for the nominal and adaptive cases. This figure clearly demonstrates that utilizing the adaptive controller results in a considerable attenuation of in the major RRO components. The 3σ of PES signal is computed for both cases and the results show that the adaptive algorithm boosts the track following performance by 22.3 percent. Figure. 11 shows the evolution of the estimated parameters. It is clear that most of the parameters have converged after 16 revolutions. However to reach the desired performance level, the adaptation continues for approximately 26 revolutions. Figure. 12 shows the adaptive step size μ_k and V_k^h (defined in (12)) of the system during this experiment. It shows that the algorithm adapts parameters until V_k^h meets the desired level – i.e. V^d – and then adaptation stops since $\mu_k = 0$. The upper bound of the dead band is defined by

$$V^{ub} := \mu^{ub}/\rho + V^d.$$

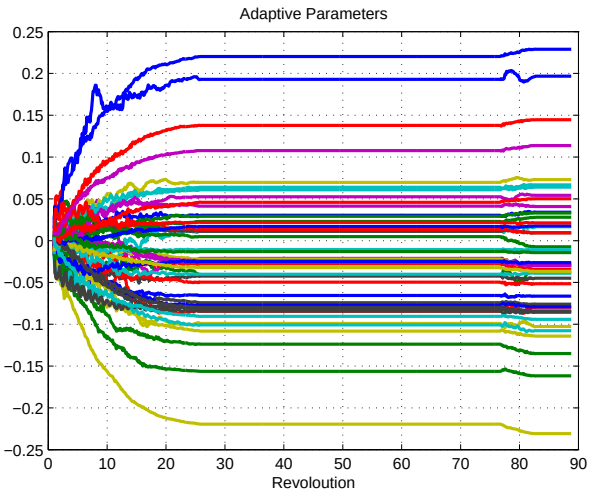

FIGURE 11: EVOLUTION OF THE ESTIMATED PARAMETERS

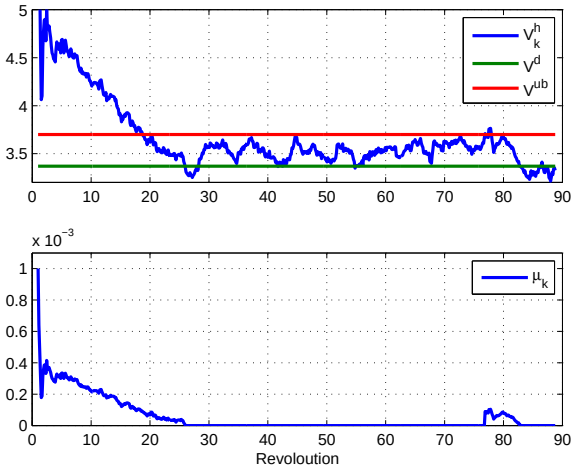

FIGURE 12: AUXILIARY ERROR POWER AND VARIABLE STEP SIZE IN 90 REVOLUTIONS OF THE DISK (EXPERIMENTS).

As mentioned earlier, if either the disturbance of plant dynamics changes such that V_k^h exceeds the upper bound, the the algorithm will re-adapt the parameters base on the new working conditions. This has happened in our system in revolution 76 where the adaptation has started automatically and has corrected the parameters very quickly.

Acknowledgment

The authors gratefully acknowledge financial support from Advanced Storage Technology Consortium (ASTC) and thank Toshiki Hirano, Tetsuo Semba, Xiaotian Sun and Philip Steiner for helpful conversations.

REFERENCES

[1] T. Inoue, M. Nakano, T. Kubo, S. Matsumoto, and H. Baba, "High accuracy control of a proton synchrotron magnet power supply," in *Proceedings of the 8th World Congress of IFAC*, vol. 20, pp. 216–221, 1981.

[2] M. Tomizuka, T.-C. Tsao, and K.-K. Chew, "Analysis and synthesis of discrete-time repetitive controllers," *Journal of Dynamic Systems, Measurement, and Control*, vol. 111, no. 3, pp. 353–358, 1989.

[3] C. Kempf, W. Messner, M. Tomizuka, and R. Horowitz, "Comparison of four discrete-time repetitive control algorithms," *IEEE Control Systems Magazine*, vol. 13, no. 6, pp. 48–54, 1993.

[4] K.-K. Chew and M. Tomizuka, "Digital control of repetitive errors in disk drive systems," in *American Control Conference, 1989*, pp. 540–548, IEEE, 1989.

[5] W. Messner, R. Horowitz, W.-W. Kao, and M. Boals, "A new adaptive learning rule," *Automatic Control, IEEE Transactions on*, vol. 36, no. 2, pp. 188–197, 1991.

[6] B. WIDROW, M. E. HOFF, *et al.*, "Adaptive switching circuits.," 1960.

[7] P. S. Diniz, *Adaptive filtering*. Springer, 1997.

[8] S. Elliott and P. Nelson, "The application of adaptive filtering to the active control of sound and vibration," *NASA STI/Recon Technical Report N*, vol. 86, p. 32628, 1985.

[9] J. C. Burgess, "Active adaptive sound control in a duct: A computer simulation," *The Journal of the Acoustical Society of America*, vol. 70, no. 3, pp. 715–726, 1981.

[10] B. Widrow, S. Shaffer, and D. Shur, "On adaptive inverse control'," in *Proc. 15th ASILOMAR Conf. on Circuits, systems and computers*, 1981.

[11] D. R. Morgan, "An analysis of multiple correlation cancellation loops with a filter in the auxiliary path," *Acoustics, Speech and Signal Processing, IEEE Transactions on*, vol. 28, no. 4, pp. 454–467, 1980.

[12] E. Bjarnason, "Noise cancellation using a modified form of the filteredxlms algorithm," *Proc. Eusipco Signal Processing V, Bnissel*, 1992.

[13] I.-S. Kim, H.-S. Na, K.-J. Kim, and Y. Park, "Constraint filtered-x and filtered-u least-mean-square algorithms for the active control of noise in ducts," *The Journal of the Acoustical Society of America*, vol. 95, no. 6, pp. 3379–3389, 1994.

[14] R. L. White, R. Newt, and R. F. W. Pease, "Patterned media: A viable route to 50 gbit/in 2 and up for magnetic record-

ing?," *Magnetics, IEEE Transactions on*, vol. 33, no. 1, pp. 990–995, 1997.

[15] C. A. Ross, "Patterned magnetic recording media," *Annual Review of Materials Research*, vol. 31, no. 1, pp. 203–235, 2001.

[16] G. Ungerboeck, "Theory on the speed of convergence in adaptive equalizers for digital communication," *IBM Journal of Research and Development*, vol. 16, no. 6, pp. 546–555, 1972.

[17] B. Widrow, J. M. McCool, M. Larimore, and C. R. Johnson, "Stationary and nonstationary learning characteristics of the lms adaptive filter," *Proceedings of the IEEE*, vol. 64, no. 8, pp. 1151–1162, 1976.

[18] A. Feuer and E. Weinstein, "Convergence analysis of lms filters with uncorrelated gaussian data," *Acoustics, Speech and Signal Processing, IEEE Transactions on*, vol. 33, no. 1, pp. 222–230, 1985.

[19] P. A. Lopes and M. S. Piedade, "The behavior of the modified fx-lms algorithm with secondary path modeling errors," *Signal Processing Letters, IEEE*, vol. 11, no. 2, pp. 148–151, 2004.

[20] L. Eriksson and M. Allie, "Use of random noise for online transducer modeling in an adaptive active attenuation system," *The Journal of the Acoustical Society of America*, vol. 85, no. 2, pp. 797–802, 1989.

[21] M. T. Akhtar, M. Abe, and M. Kawamata, "A new variable step size lms algorithm-based method for improved online secondary path modeling in active noise control systems," *Audio, Speech, and Language Processing, IEEE Transactions on*, vol. 14, no. 2, pp. 720–726, 2006.

[22] A. Al Mamun, G. Guo, and C. Bi, *Hard disk drive: mechatronics and control*, vol. 23. CRC PressI Llc, 2007.

[23] A. H. Sacks, M. Bodson, and W. Messner, "Advanced methods for repeatable runout compensation [disc drives]," *Magnetics, IEEE Transactions on*, vol. 31, no. 2, pp. 1031–1036, 1995.

[24] S.-C. Wu and M. Tomizuka, "Repeatable runout compensation for hard disk drives using adaptive feedforward cancellation," in *American Control Conference, 2006*, pp. 6–pp, IEEE, 2006.

[25] Y. Q. Chen, K. L. Moore, J. Yu, and T. Zhang, "Iterative learning control and repetitive control in hard disk drive industry-a tutorial," in *Decision and Control, 2006 45th IEEE Conference on*, pp. 2338–2351, IEEE, 2006.